

TripleE: Easy Domain Generalization via Episodic Replay

Xiaomeng Li · Hongyu Ren · Huifeng Yao · Ziwei Liu

Received: date / Accepted: date

Abstract Learning how to generalize the model to unseen domains is an important area of research. In this paper, we propose TripleE, and the main idea is to encourage the network to focus on training on subsets (learning with replay) and enlarge the data space in learning on subsets. Learning with replay contains two core designs, EReplayB and EReplayD, which conduct the replay schema on batch and dataset, respectively. Through this, the network can focus on learning with subsets instead of visiting the global set at a glance, enlarging the model diversity in ensembling. To enlarge the data space in learning on subsets, we verify that an exhaustive and singular augmentation (ESAug) performs surprisingly well on expanding the data space in subsets during replays. Our model dubbed **TripleE** is frustratingly easy, based on simple augmentation and ensembling. Without bells and whistles, our TripleE method surpasses prior arts on six domain generalization benchmarks, showing that this approach could serve as a stepping stone for future research in domain generalization.

Keywords Domain generalization · Augmentation · Learning with replay

Xiaomeng Li
The Hong Kong University of Science and Technology
E-mail: eexmli@ust.hk

Hongyu Ren
Stanford University
E-mail: hyren@cs.stanford.edu

Huifeng Yao
The Hong Kong University of Science and Technology
E-mail: hyaoad@connect.ust.hk

Ziwei Liu
S-Lab, Nanyang Technological University, Singapore
E-mail: ziwei.liu@ntu.edu.sg

1 Introduction

Deep neural networks have achieved remarkable success on various computer vision tasks [15, 36, 22, 66, 34] with an assumption that the training and test datasets consist of *i.i.d.* samples from the same distribution. However, in real-world scenarios, the test data (target domain) are often outside the training dataset domains (source domains), posing a significant challenge to deep learning algorithms. Domain generalization (DG) assumes that a model is trained from multiple source domains and expected to perform well on unseen domains. In such scenarios, the model inherently cannot capture any distribution shift between the source and target domains. Thus, a robust training method is crucial to domain generalization tasks.

Recent studies on DG have explored several directions, and these methods can be broadly classified into three categories: 1) Learning domain-invariant representation [58, 10, 3, 32], which aims to learn a shared domain-invariant representation for images from multiple source domains. 2) General model regularization [24, 49, 57], which imposes additional regularization terms upon the model during training, *e.g.*, gradient dropouts [24], informative dropout [49] and superficial information regularization [57]. 3) Augmenting source domains [55, 51, 64, 33, 60], whose goal is to enlarge the training data to a broader span of the data space, increasing the possibility of covering the data in the target domain. Although prior works have achieved promising results, most methods are complicated, containing hand-crafted architectures, memory banks, multiple training stages, or self-supervised tasks [3, 58, 7]. For example, Chen *et al.* [7] proposed a style and semantic memory mechanism, which requires building multi-

ple memory banks to store style and semantic features. Xu *et al.* [60] proposed a Fourier transformation for DG based on a teacher-student model.

Unlike prior work, we propose a frustratingly easy and powerful baseline method for domain generalization with simple augmentation and ensembling. We discover a key insight of DG is to encourage the network to *focus on training on subsets (learning with replay)* and *enlarge the data space in performing replays*. The *subsets* should belong to the whole set and can be defined on *batch* and on *dataset* level. Therefore, learning with replay has two core designs: **1) Episodic replay on batch (EReplayB)**: augment each batch multiple times. By augmenting *batch* multiple times, EReplayB encourages the network to focus on learning with *subsets (batch)*. **2) Episodic replay on dataset (EReplayD)**: randomly split the dataset into sub-datasets, train models on sub-datasets individually, periodically resplit sub-datasets, and ensemble the predictions of models trained with sub-datasets. To enlarge the data space in learning on *subsets*, we further introduce **3) Exhaustive, and singular augmentation (ESAug)**: a cascade of successive compositions can produce images that drift far from the original image and lead to unrealistic images. Unlike prior work, we employ exhaustive and singular augmentation to enhance the generalization.

Overall, EReplayB and ESAug work well because they can effectively decrease gradient variance reduction in each optimization step, could help the model avoid sharp minima, and reach a more robust solution. EReplayD enforces the model to learn with sub-datasets instead of visiting the whole set at a glance, and the model has the chance to visit the whole set because of periodic updates of sub-datasets. Therefore, it can generate more diverse models and is demonstrated to be more effective than the traditional ensembling method.

The main contributions of this paper are listed as follows:

- We reveal a key secret for the performance gains is to encourage the network to train with subsets and enlarge the data space in learning on subsets. This simple but overlooked point should be known in the fast-growing DG area.
- We propose TripleE, which consists of three components: EReplayB, EReplayD, and ESAug. EReplayB and EReplayD perform *learning with replay* on batch and dataset, respectively. ESAug can effectively *enlarge the data space during replays*.
- Without bells and whistles, TripleE outperforms other state-of-the-art methods on six DG benchmarks, notably achieving 5.54% and 2.23% improvements on Digits-DG and PACS, respectively, showing that our method could serve as a stepping stone for future research in domain generalization ¹.

2 Related Work

Considerable efforts have been devoted to DG to design models which reduce reliance on domain-specific artifacts. In the following, we review the related DG literature from three perspectives. Furthermore, we discuss some related approaches on batch training techniques and augmentations.

DG via Learning Domain-invariant Representation. The research in this direction aims to learn domain-invariant representation by minimizing the discrepancy between source domains [16, 41, 29, 30, 31, 10, 32]. The resulting domain-invariant representation can then be used for downstream tasks in the unseen target domain. Along this track, Ghifary [16] designed a multi-task autoencoder, which transfers an image to its related domains and thereby learns robust representation across various domains. Another related work is the maximum mean discrepancy-based adversarial autoencoder (MMD-AAE) [32], which applies MMD distance to align the distributions among different domains via adversarial training [17]. However, these methods require the source domain partitions.

Recent DG methods forgo the requirement of source domain partitions and directly learn with the mixed domains of training data. Some methods designed additional regularizations for learning invariant representation. For example, JiGen [3] developed a self-supervised task, solving jigsaw puzzles, to capture the invariant information within images from multiple source domains. Instead of only capturing invariance within a single image, Wang *et al.* [58] proposed to learn an extrinsic relationship among images across domains to improve generalization.

DG via General Model Regularization. The research in this line considers improving domain generalization through reducing the factor of superficial information on the model prediction [57, 56, 24, 49]. For example, Wang *et al.* [57] proposed to reduce the model’s reliance on known superficial information such as irrelevant textures and encourage the model to rely more on

¹ Code is available at <https://github.com/xmed-lab/TripleE-DG>

informative parts. Some Dropout-like algorithms [52] are also introduced to solve the DG problem [49, 22]. Shi *et al.* [49] designed an InfoDrop to improve the model generalization by reducing model bias to texture.

DG via Augmenting Source Domain. Since no information from the target domain is available during training, some researchers proposed to generate synthetic images derived from multiple source domains to increase the diversity of the training data [62, 61, 48, 55, 64, 51, 60]. By augmenting the source domain data, the model has a broader range of visible domains and a higher possibility of covering the span of target data. For example, Yue *et al.* [61] proposed to augment the training data by randomizing the synthetic images with the styles of real images from auxiliary datasets.

Our method belongs to the augmentation-based method. Unlike the above methods, we present a frustratingly easy domain generalization based on simple augmentation and ensembling. We point out an important insight for DG via augmentations, that is, learning with replay on *subsets* and enlarging the data space when performing replays. However, this simple yet effective point has been overlooked in prior work and should be known given the recent progress in domain generalization.

Batch Training and Augmentation. Outside the literature of domain generalization, many recent works studied several general techniques for improved batch training and augmentation, which go beyond augmenting source domain data [21, 25, 39]. For example, Hoffer *et al.* [21] proposed adding repetitive data to a batch to improve robustness in a supervised learning setting. Many other researchers developed various automated data augmentation methods [8, 37, 9, 42] to define different augmentation search policies and strategies. In contrast, this paper reveals a key idea to generalization improvements but neglected in prior work: learning with replay and enlarging the data space when performing replays.

3 Our Approach

We denote $\mathcal{D} = \{(\mathbf{x}_i, y_i)\}_{i=1}^N$ as a mixed training dataset from multiple source domains, consisting of N image-label pairs, where y_i denotes the class label of image \mathbf{x}_i . Note we do not assume we have access to the domain label, *i.e.*, which source domain a given \mathbf{x}_i belongs to. The goal in DG is to learn a domain-generalized network $f_\theta(\cdot)$ from the source domains and test it on an unseen target domain. Fig. 1 shows an illustration of TripleE.

3.1 EReplayB: Episodically Replay on Batch

The main idea of EReplayB is to episodically replay each training sample in a batch, and it works as follows. Let $\mathcal{B} \subseteq \mathcal{D}$ denote a set of randomly sampled images during training, where the cardinal number of set \mathcal{B} is batch size b . We denote a set of augmentations as \mathcal{A} , where $\mathcal{A} = \{a_1, a_2, \dots, a_n\}$. The standard operation in many DG methods [3, 60, 58] is to sequentially apply each augmentation function with some randomness to an input image and the perturbed image can be described as $(a_n \dots a_3(a_2(a_1(\mathbf{x}_i))))$. We introduce EReplayB to episodically replay each sample in a batch. Specifically, each sample in \mathcal{B} is augmented by r different transformations from \mathcal{A} . As a result, we can obtain an augmented sample set, denoted as \mathcal{B}' and $|\mathcal{B}'| = r|\mathcal{B}|$.

As each batch contains multi-views for a single image, it is natural to include positive pairs, which motivates us to leverage the supervised contrastive loss [26]. Unlike existing methods designed complicated self-learning loss [3, 58], we use a simple weighted combination of a standard cross-entropy loss and a supervised contrastive loss. We denote $\mathcal{P}(i) = \{j \in [0, |\mathcal{B}'|] \mid y_j = y_i, j \neq i\}$ as the set of indices of all positives (with the same label) in the batch \mathcal{B}' distinct from i and $|\mathcal{P}(i)|$ is its cardinality. Note that we guarantee that $\forall i, |\mathcal{P}(i)| \geq r - 1$ since each sample is replayed in the updated batch \mathcal{B}' . The positive pairs in the batch include the augmented views of image \mathbf{x}_i and may also contain other image samples with the same label with image \mathbf{x}_i from the current or different source domains. The negative pairs in the batch are images with different labels.

$$\ell_{sup} = - \sum_i \frac{1}{|\mathcal{P}(i)|} \sum_{j \in \mathcal{P}(i)} \log\left(\frac{\exp(s_{i,j}/\tau)}{\sum_{k=1}^{r \cdot |\mathcal{B}|} \mathbb{1}_{[k \neq i]} \exp(s_{i,k}/\tau)}\right), \quad (1)$$

where $\tau > 0$ is the temperature; $s_{i,j}, s_{i,k}$ denote the feature similarities among positive pairs and negative pairs, respectively; $r \cdot |\mathcal{B}|$ is the size of the sample set \mathcal{B}' . The total objective is

$$\ell = \ell_{ce} + \ell_{sup}, \quad (2)$$

where ℓ_{ce} refers to a standard cross-entropy loss. It is worth mentioning that the performance gains of EReplayB are mainly from episodically replaying of the image sample (+4.78% Acc.), instead of the contrastive loss (+0.74% Acc.); see results in Table 5.

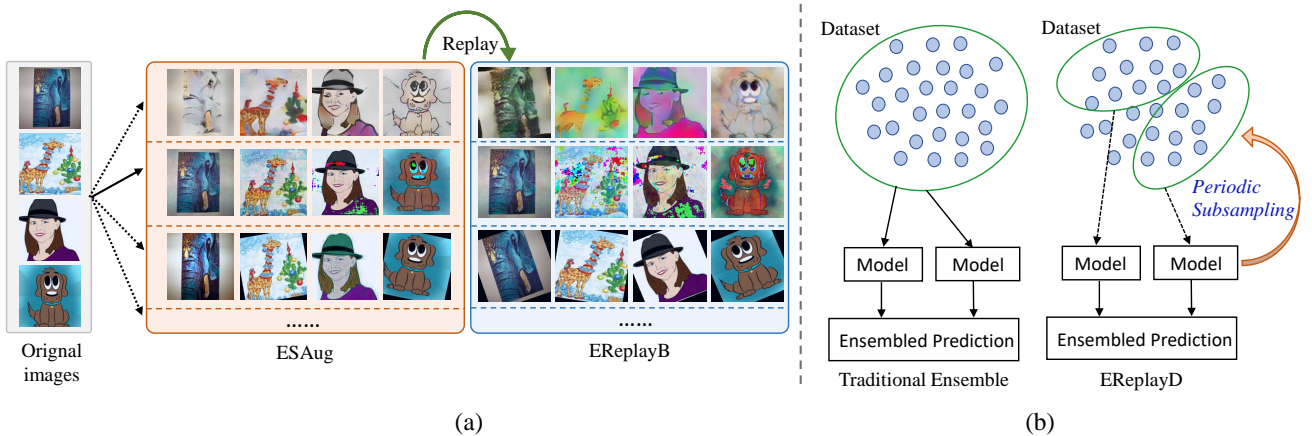


Fig. 1: Illustration of TripleE: (a) EReplayB and ESAug. (b) Traditional ensemble vs. EReplayD.

3.2 ESAug: Exhaustive and Singular Augmentation

ESAug enlarges the data space when performing EReplayB and EReplayD. It highlights two core questions: (1) what should be included in the transformation list when performing replays and (2) how to perform augmentation?

First, we empirically demonstrated that the augmentation should consist of exhaustive transformation functions when learning with replays. We let the augmentation set \mathcal{A} to include transformations defined in [9], each of which can generate a set of distortions to an image. However, these augmentations only perform transformations within a single image. To improve model generalization, we enlarge \mathcal{A} to \mathcal{A}' by introducing two cross-image augmentations (Fourier-based augmentation and Style-based augmentation) to encourage the network to learn high-level semantics by exchanging the low-level statistics among images in the source domains.

Fourier-based augmentation. Considering that the Fourier phase component contains some semantic-preserving (high-level) information, augmenting the training data by distorting the amplitude information while keeping the phase information unchanged is a good way for the model to learn robust features. Through a Fourier-based augmentation, our model can avoid overfitting to low-level statistics carried in the amplitude information, thus paying more attention to the phase information when making decisions. Specifically, we employ a Fourier-based augmentation by linearly interpolating between the amplitude spectrums of two images from arbitrary source domains:

$$\hat{\mathcal{T}}(x_i) = (1 - \lambda)\mathcal{T}(x_i) + \lambda\mathcal{T}(x_j), \quad (3)$$

```

within_image_tr = ['Identity', 'AutoContrast', 'Equalize', 'Rotate', 'Solarize', 'Color', 'Posterize', 'Contrast',
                  'Brightness', 'Sharpness', 'ShearX', 'ShearY', 'TranslateX', 'TranslateY']
cross_images_stylizedtr = ['Stylized']
cross_images_fouriertr = ['Fourier']
def ESAug(s):
    """Generate a set of within-image and cross-image distortions.
    Args: s: Strength for the selected transformation.
    """
    transforms = np.concatenate([within_image_tr, cross_images_stylizedtr]) # Stylized version
    # transforms = np.concatenate([within_image_tr, cross_images_fouriertr]) # Fourier version

    sampled_ops = np.random.choice(transforms, 1)
    return (sampled_ops, s)

```

Fig. 2: Python code for ESAug based on numpy.

where $\mathcal{T}(x_i)$ refers to amplitude component of image x_i calculated by FFT [45] algorithm. $\lambda \sim U(0, \xi)$ and hyperparameter ξ controls the strength of the augmentation. The mixed amplitude spectrum is then combined with the original phase spectrum to form a new Fourier representation:

$$\mathcal{F}(\hat{x}_i)(u, v) = \hat{\mathcal{T}}(x_i)(u, v) * e^{-i*\mathcal{P}(x_j)(u, v)}, \quad (4)$$

where $\mathcal{P}(x_i)$ refers to phase component. Then, the augmented image can be described as

$$\hat{x}_i = \mathcal{F}^{-1}[\mathcal{F}(\hat{x}_i)(u, v)]. \quad (5)$$

We denote the set \mathcal{A}^f to represent the transformation from x_i to \hat{x}_i . The final augmentation set can be defined as \mathcal{A}' and $\mathcal{A}' = \mathcal{A} \cup \mathcal{A}^f$.

Style-based augmentation. The core idea of style-based augmentation is motivated by the fact that different domains contain different style information. To learn domain-invariant features, a good model should be invariant to style changes among domains. To achieve it, we include a random stylization as an augmentation to enhance the network. Specifically, we use

Algorithm 1 TripleE for Domain Generalization

Require: Source domains \mathcal{D} , batch size b , replay times r , sub-sampling times m

Require: m neural networks that share a same structure $f_1(\theta), \dots, f_m(\theta)$

Require: A set of exhaustive augmentations \mathcal{A}'

- 1: **while** not converged **do**
- 2: Initialize model parameters for $f_1(\theta), \dots, f_m(\theta)$
- 3: **for** epochs = 1 to N **do**
- 4: Randomly split \mathcal{D} into D^1, D^2, \dots, D^m # EReplayD

- 5: **for** each sub-dataset D^i in \mathcal{D} **do**
- 6: **for** each step **do**
- 7: Sample \mathcal{B} from D^i
- 8: Sample an augmentation a from \mathcal{A}' # ESAug

- 9: Sample a strength s from $\{0, \dots, 30\}$
- 10: Obtain \mathcal{B}' by augmenting \mathcal{B} with r different transformations from \mathcal{A}' , where each augmentation is $a(x, s)$ # EReplayB
- 11: Optimize $f_i(\theta)$ using Eq. 2.
- 12: **end for**
- 13: **end for**
- 14: **end for**
- 15: **end while**
- 16: **return** $\theta_1, \dots, \theta_m$

a pre-trained AdaIN [23] which can achieve fast stylization to arbitrary styles. We randomly sample an image x_j from source domains and $y_j = y_i$. Then, we randomly stylize an image x_i with the style of x_j and obtain \hat{x}_i . We denote the set \mathcal{A}^s to represent the transformation from x_i to \hat{x}_i . The final augmentation set can be defined as \mathcal{A}' and $\mathcal{A}' = \mathcal{A} \cup \mathcal{A}^s$.

Singular Augmentation Second, we verified that the learning with replay should be performed with a randomly selected transformation from the augmentation list with some randomness instead of sequentially applying several transformation functions. Prior work also observed that a cascade of successive compositions could produce images that drift far from the original image and lead to unrealistic images [20]. Therefore, we randomly select a singular augmentation from the augmentation list. Due to the design of singular augmentation, we randomly set parameter ξ in Fourier-based augmentation to increase some randomness to the augmentation strength, which is different from the fixed ξ and a sequential augmentation in [60]. For style-based augmentation, we increase the augmentation randomness by randomly choosing an image from the dataset as the target to stylize image x_i . Fig. 2 shows Python code for ESAug based on numpy.

3.3 EReplayD: Episodically Replay on Dataset

The idea of learning with replay is further performed on a sub-dataset, namely EReplayD. The key motiva-

tion of EReplayD is that learning with periodic updates of subsets can achieve more diverse models, leading to an improved model ensemble. Specifically, instead of training a model on a whole training dataset \mathcal{D} , EReplayD randomly splits the training dataset \mathcal{D} into m sub-datasets D^1, D^2, \dots, D^m and trains m models on each sub-dataset. Note that the dataset will be randomly split into m sub-datasets every epoch such that each model can focus on learning each sub-dataset while keeping a chance to visit the overall dataset. The final prediction will be an ensemble of predictions from m models. Fig. 1(b) shows the comparison of the traditional model ensemble and our EReplayD. Algorithm 1 shows the overall training pipeline of TripleE.

4 Experiments

4.1 Datasets and Settings

Datasets. We evaluate our method on six widely-used datasets in domain generalization, *i.e.*, **Digits-DG**, **PACS** and **Office-Home**, **VLCS**, **TerraInc** and **DomainNet**. Digits-DG [64] contains four different digit datasets, *i.e.*, MNIST [28], MNIST-M [13], SVHN [43], and SYN [13]. PACS [29] contains 9,991 images of four domains (Artpaint, Cartoon, Sketches, and Photo) and 7 classes. Office-Home [54] contains 15,558 images of 65 classes, distributed across 4 domains (Artistic, Clipart, Product, and Real world). VLCS [12] includes photographic domains (Caltech101, LabelMe, SUN09, VOC2007) with 10,729 images and 5 classes. TerraInc dataset [2] contains 24,788 images with 10 classes over 4 domains. DomainNet dataset [47] has 586,575 images with 345 classes over 6 domains.

Evaluation protocol. Following prior works [60, 3], we train our model on the training splits and select the best model on the validation splits of all source domains. For testing, we evaluate the selected model on all images of the held-out target domain. For performance evaluation, we report top-1 classification accuracy on each test domain and average accuracy accordingly.

4.2 Implementation Details

Here we briefly introduce the main details for training our method.

Basic details: All experiments were implemented in PyTorch [46] and run on a machine with an NVIDIA RTX 3090 GPU. We trained all the models with the

Table 1: Domain generalization results on the Digits-DG dataset (Backbone: 4 conv layer, which is used in [64]). “DL” refers to using domain label or not.

	DL	SYN	SVHN	MNIST-M	MNIST	Avg.
Vanilla [63]	✗	78.6	61.7	58.8	95.8	73.7
CCSA [41]	✓	79.1	65.5	58.2	95.2	74.5
MMD-AAE [32]	✓	78.4	65.0	58.4	96.5	74.6
CrossGrad [48]	✓	80.2	65.3	61.1	96.7	75.8
DDAIG [63]	✓	81.0	68.6	64.1	96.6	77.6
L2A-OT [64]	✓	83.2	68.6	63.9	96.7	78.1
STEAM [7]	✓	92.2	76.0	67.5	96.8	83.1
JiGen [3]	✗	74.0	63.7	61.4	96.5	73.9
SFA [33]	✗	85.0	70.3	66.5	96.5	79.6
FACT [60]	✗	90.3	72.4	65.6	97.9	81.5
TripleE-Style (ours)	✗	95.33	81.75	72.52	98.28	86.97
TripleE-Fourier (ours)	✗	95.48	81.22	73.15	98.33	87.04

cross-entropy loss and an InfoNCE loss function [26]. For Digits-DG, we use the same backbone network as [64, 3]. We train the network from scratch using SGD and the initial learning rate is set to 0.01. For PACS and Office-Home, we use ImageNet pretrained ResNet [19] as our backbone. The initial learning rate of PACS is 0.0001 and decayed by 0.5 every 30 epochs. The initial learning rate of Office-Home is 0.01 and decayed by 0.5 every 30 epochs. The network is totally trained for 100 epochs as [58]. For VLCS and TerraInc, we use the ImageNet pretrained ResNet-50 [19] as our backbone. The initial learning rate is 0.001 and decayed by 0.5 every 40 epochs. We trained 100 epochs for these two datasets. For DomainNet, we also use the ImageNet pretrained ResNet-50 [19] as our backbone. The initial learning rate is 0.001 and decayed by 0.5 every 16 epochs. We trained 40 epochs for this dataset.

Method-specific details: For Digits-DG and PACS, both batch size b and repeat time r are set to 4. For Office-Home, both b and r are set to 32. For VLCS, TerraInc, and DomainNet, the batch size b is 16, and the repeat time r is 4. For all experiments, we set the sampling times m to 3.

4.3 Evaluation on six DG benchmarks

Digits-DG dataset. Table 1 shows the results on the Digits-DG dataset. It is clear that our TripleE method outperforms the prior state-of-the-art DG methods STEAM [7] and FACT [60] by an average of 3.9% and 5.5% on top-1 classification accuracy, respectively. Please note that STEAM [7] not only requires domain label information but also requires carefully designing a teacher-student model and multiple memory banks to store the style features for each source domain. In contrast, our TripleE method does not require a domain label and does not need any particular architecture design. Using simple data augmentation and sub-sampling

Table 2: Domain generalization results on the PACS dataset. “S,C,A,P” refer to “Sketch, Cartoon, Art painting, and Photo”, respectively. Each reported result of our method is averaged over three runs. †use *test-domain-validation-set*, where some target images are used to select the best model. “DL” refers to using domain label or not.

	DL	S	C	A	P	Avg.
ResNet-18						
Vanilla	✗	69.64	75.65	77.38	94.25	79.23
MMD-AAE [32]	✓	64.2	72.7	75.2	96.0	77.0
CCSA [41]	✓	66.8	76.9	80.5	93.6	79.4
D-SAM [11]	✓	77.83	72.43	77.33	95.30	80.72
MASF [10]	✓	71.69	77.17	80.29	94.99	81.04
DMG [6]	✓	75.21	80.38	76.90	93.35	81.46
Epi-FCR [31]	✓	73.0	77.0	82.1	93.9	81.5
CuMix [38]	✓	72.6	76.5	82.3	95.1	81.6
MetaReg [1]	✓	70.3	77.2	83.7	95.5	81.7
L2A-OT [64]	✓	73.6	78.2	83.3	96.2	82.8
SelReg [27]	✓	77.47	78.43	82.34	96.22	83.62
STEAM [7]	✓	82.9	80.6	85.5	97.5	86.6
JiGen [3]	✗	71.35	75.25	79.42	96.03	80.51
SFA [33]	✗	73.7	77.8	81.2	93.9	81.7
MMLD [40]	✗	72.29	77.16	81.28	96.09	81.83
EISNet [58]	✗	74.33	76.44	81.89	95.93	82.15
InfoDrop [49]	✗	76.38	76.54	80.27	96.11	82.33
pAdaIN [44]	✗	75.13	76.91	81.74	96.29	82.51
FACT [60]	✗	79.15	78.38	85.37	95.15	84.51
TripleE-Style (ours)	✗	84.53	81.02	85.16	96.23	86.74
TripleE-Fourier (ours)	✗	84.45	80.84	85.3	96.27	86.72
ResNet-50						
Vanilla	✗	69.69	78.61	81.47	94.83	81.15
MASF [10]	✓	72.29	80.49	82.89	95.01	82.67
MetaReg [1]	✓	70.30	79.20	87.20	97.60	83.60
DMG [6]	✓	78.32	78.11	82.57	94.49	83.37
pAdaIN [44]	✗	77.37	81.06	85.82	97.17	85.36
EISNet [58]	✗	78.07	81.53	86.64	97.11	85.84
Contrastive ACE [59] †	✗	80.6	81.9	88.8	97.7	87.3
SWAD [4]	✗	-	-	-	-	88.1
FACT [60]	✗	84.46	81.77	89.63	96.75	88.15
TripleE-Style (ours)	✗	88.19	85.2	90.97	97.72	90.52
TripleE-Fourier (ours)	✗	86.23	85.37	91.06	98.32	90.25

ensemble, our method can achieve the best performance. Notably, FACT [60] is a dual-model (teacher-student model) that relies on Fourier transforms to exchange domain information. However, our TripleE model obtains significant improvements (+8.82% and +7.55% on SVHN and MNIST-M, respectively) over FACT [60]. The result demonstrates that our simple approach can effectively deal with large domain shifts caused by complex backgrounds and cluttered digits.

PACS dataset. Table 2 shows the results on the PACS dataset. We can see that our TripleE can clearly outperform the prior best DG method under the same setting by 2.2% and 2.4% using ResNet-18 and ResNet-50, respectively. Notably, TripleE-Style and TripleE-Fourier can reach comparable performance on both PACS and Digits-DG, showing that these two kinds of augmentation can encourage the network to learn high-level semantics by exchanging low-level statistics among images. Note that FACT [60] built a dual-model (teacher-student models) and encourages high-level semantic exchanges among domains to improve generalization. Un-

Table 3: Domain generalization results on the Office-Home dataset. “DL” refers to using domain label or not (Backbone: resnet-18).

	DL	Art	Clipart	Product	Real World	Avg.
Vanilla [63]	✗	58.9	49.4	74.3	76.2	64.7
MMD-AAE [64]	✓	56.5	47.3	72.1	74.8	62.7
CrossGrad [48]	✓	58.4	49.4	73.9	75.8	64.4
CCSA [41]	✓	59.9	49.9	74.1	75.7	64.9
DDAIG [41]	✓	59.2	52.3	74.6	76.0	65.5
L2A-OT [64]	✓	60.6	50.1	74.8	77.0	65.6
STEAM [7]	✓	62.1	52.3	75.4	77.5	66.8
JiGen [3]	✗	53.0	47.5	71.5	72.8	61.2
RSC [24]	✗	74.54	71.63	47.90	58.42	63.12
FACT [60]	✗	60.34	54.85	74.48	76.55	66.56
TripleE-Style (ours)	✗	63.10	56.47	76.10	76.42	68.02
TripleE-Fourier (ours)	✗	62.59	57.55	75.69	77.48	68.33

like this method, our TripleE is a simple augmentation and ensemble method. It is worth mentioning that SFA [33] is also an augmentation-based method that augments feature embeddings to improve domain generalization. However, in terms of accuracy, our method can excel all other DG methods and reach a comparable performance with STEAM [7], which uses domain labels and builds a complex network with at least three memory banks.

Office-Home dataset. The results are shown in Table 3. Notably, a simple vanilla model shows strong results on this benchmark. Most baselines provide only marginal improvements to the vanilla model with less than 1.0% improvements. One reason is that Office-Home is a relatively large composition of data, compared with PACS and Digits-DG, thus offering inherently bigger domain diversity in training data already [64]. Overall, our TripleE can surpass the best DG method FACT [60] and STEAM [7] by 1.77% and 1.53%, respectively. The state-of-the-art result on Office-Home dataset further validates the effectiveness of our proposed EReplayB, ESAug, and EReplayD.

VLCS, TerraInc and DomainNet datasets. Table 4 shows the comparison with existing state-of-the-arts on multiple DG benchmarks. SWAD [4] is one of the existing DG methods. In all experiments, our TripleE achieves significant performance gain against the previous best method SWAD [4]. The comparison shows that our TripleE could serve as a stepping stone for future research in domain generalization.

4.4 Ablation Studies

Ablation of our baseline model. We first point out that there are several inconsistent baselines in DG that share the same network structures but employ different augmentations. As shown in Table 5, early DG methods [63,3] use random crop, and random horizontal

Table 4: Comparisons of results on PACS, VLCS, OfficeHome, TerraInc, and DomainNet. Except for our method, other results are adopted from [4].

	Avg.	PACS	VLCS	OfficeHome	TerraInc	DomainNet
Mixstyle [65]	60.3	85.2	77.9	60.4	44.0	34.0
C-DANN [35]	62.6	82.8	78.2	65.6	47.6	38.9
DANN [14]	63.1	84.6	78.7	65.4	48.4	38.4
ERM [18]	63.8	85.7	77.4	67.5	47.2	41.2
Fish [50]	63.9	85.5	77.8	68.6	45.1	42.7
CORAL [53]	64.1	86.0	77.7	68.6	46.4	41.8
MIRO [5]	65.9	85.4	79.0	70.5	50.4	44.3
SWAD [4]	66.9	88.1	79.1	70.6	50.0	46.5
TripleE (ours)	69.1	90.5	80.1	74.0	52.7	48.2

Table 5: Effectiveness of different components on Digits-DG, PACS, and Office-Home datasets (Backbone: ResNet-18). Vanilla refers to baseline used in early DG methods [63,3]. Compared to Vanilla, recent DG methods [58,60] use Baseline† that additionally employs color jittering as the basic data augmentation. Baseline(ours) keeps consistent with Baseline† except for an additional contrastive loss [26].

Digits-DG dataset								
	EReplayB	ESAug	EReplayD	SYN	SVHN	MNIST-M	MNIST	Avg.
Vanilla [3,63]	-	-	-	78.6	61.7	58.8	95.8	73.7
Baseline† [58,60]	-	-	-	89.93	64.43	58.32	95.8	77.12
Baseline (ours)	-	-	-	90.63	66.58	58.68	95.55	77.86
Model a	✓	-	-	92.8	75.4	63.1	96.4	81.9
Model b	-	✓	-	93.65	74.37	63.03	97.43	82.12
Model c	-	-	✓	90.07	69.02	65.47	97.83	80.60
Model d	✓	✓	-	94.62	79.83	69.85	97.43	85.43
Model e	✓	-	✓	94.12	76.70	72.05	98.18	85.26
Model f	✓	-	✓	93.50	77.07	64.97	97.30	83.21
TripleE (ours)	✓	✓	✓	95.33	81.75	72.52	98.28	86.97
PACS dataset								
	EReplayB	ESAug	EReplayD	S	C	A	P	Avg.
Vanilla [3,63]	-	-	-	69.64	75.65	77.38	94.25	79.23
Baseline† [58,60]	-	-	-	79.74	79.26	79.49	93.41	82.98
Baseline (ours)	-	-	-	76.34	79.35	80.96	95.63	83.07
Model a	✓	-	-	82.78	78.28	84.57	95.93	85.39
Model b	✓	✓	-	84.06	80.84	83.5	95.33	85.93
TripleE (ours)	✓	✓	✓	84.53	81.02	85.16	96.23	86.74
Office-Home dataset								
	EReplayB	ESAug	EReplayD	Art	Clipart	Product	Real World	Avg.
Vanilla [3,63]	-	-	-	58.9	49.4	74.3	76.2	64.7
Baseline† [60]	-	-	-	55.34	52.46	73.01	73.17	63.50
Baseline (ours)	-	-	-	58.22	54.64	73.62	73.49	64.99
Model a	✓	-	-	60.73	53.06	73.80	75.42	65.75
Model b	✓	✓	-	59.87	58.10	75.02	75.69	67.17
TripleE (ours)	✓	✓	✓	62.59	57.55	75.69	77.48	68.33

flip as the augmentation denoted as **Vanilla**. Whereas, recent DG methods [58,60] use a stronger **Baseline†** that additionally employs color jittering as the basic data augmentation, which can enhance the performance from 73.7% to 77.1%. **Baseline(ours)** keeps consistent with **Baseline†** except for an additional contrastive loss [26]. To use the contrastive loss, we add a projection head, which sequentially consists of a fully connected layer, a batch normalization layer, a ReLU, and a fully connected layer to map the feature dimension to 128. Although with a slightly stronger baseline, we verify that the performance improvements are from our proposed TripleE instead of the baseline.

Impact of different components. Table 5 shows the effectiveness of our proposed TripleE (EReplayB, ESAug, and EReplayD). Note that all experiments used Baseline(ours) as the backbone model. From experiments on Digits-DG, we can see that EReplayB,

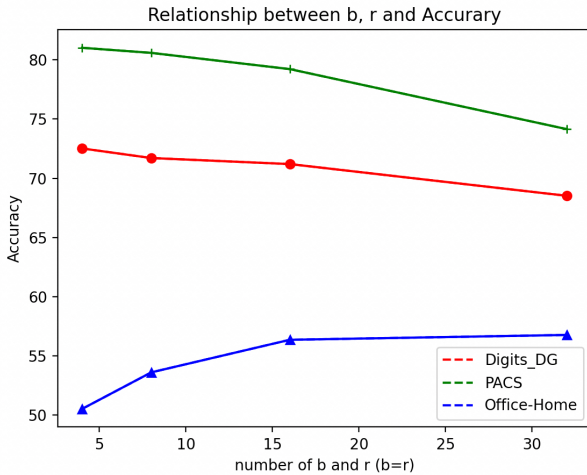


Fig. 3: Effects of different b and r in EReplayB on three datasets. The result is reported on *MNIST-M*, *Cartoon* and *Clipart* in Digits-DG, PACS and Office-Home, respectively.

ESAug, and EReplayD can enhance our baseline by 4.0%, 4.3%, 2.74%, respectively. From Model d and Model e, we can see that combing ESAug with EReplayB or EReplayD can largely improve the performance to 85.43% and 85.26%. With all these three components, our TripleE can achieve 86.97%. The result *verifies our idea that ESAug can improve generalization performance by enlarging the data space in replays*. Note that except for Model c, all other combinations of our method can excel the current best DG method FACT [60] (81.5%). For experiments on PACS and Office-Home, we can see that training with EReplayB can outperform our baseline by 2.3% and 1.7% on PACS and Office-Home, respectively. Note that compared to our baseline, EReplayB only changes the batch size b and repeat times r , showing that training with subsets can effectively improve the model generalization. By comparing **Model a** and **Model b**, we can see that using ESAug can increase the performance by 0.7% and 1.4% on PACS and Office-Home, respectively. These results demonstrated the effectiveness of enlarging data space when training with replays. Finally, we can see that using all three components can achieve the best performance on three datasets.

Ablation of EReplayB: a small batch with sufficient replay can enhance the generalization. Fig. 3 shows ablation study on parameter b and r . Here, we empirically let b equal to r and show their effects to the performance. From Fig. 3 we can see that when $b = r = 4$ in Digits-DG and PACS, our method can achieve the best performance. The result verified the effectiveness of training a small batch (sub-

Table 6: Ablation studies of ESAug on Digits-DG. \mathcal{A} refers to augmentations used in [9] and \mathcal{A}' refers to include one cross-image augmentation. “S” refers to randomly selecting a singular augmentation, and “Non-S” refers to sequentially applying augmentations.

	AugType	AugList	SYN	SVHN	MNIST-M	MNIST	Avg.
StandardAug	Non-S	\mathcal{A}	94.55	76.18	63.88	95.48	82.52
TrivialAug	S	\mathcal{A}	94.88	80.65	71.43	98.35	86.33
TripleE-Style (ours)	S	\mathcal{A}'	95.33	81.75	72.52	98.28	86.97
TripleE-Fourier (ours)	S	\mathcal{A}'	95.48	81.22	73.15	98.33	87.04

Table 7: Ablation studies on m in EReplayD on Digits-DG.

Sub-sample times	SYN	SVHN	MNIST-M	MNIST	Avg.
$m = 1$ (without EReplayD)	94.62	79.83	69.85	97.43	85.43
$m = 2$	95.48	79.75	68.7	98.08	85.50
$m = 3$	95.33	81.75	72.52	98.28	86.97
$m = 4$	94.87	79.48	70.67	98.00	85.76
$m = 5$	94.47	78.10	70.07	97.98	85.16

set) with replay (augment for multiple times). Whereas when $b = r = 32$, our method can achieve the best result on Office-Home. As b and r increase, our performance may be higher, but this experiment has a high computational cost and is left as our future work.

Ablation of ESAug: exhaustive and singular augmentation can boost the generalization. Table 6 shows the effectiveness of our ESAug in terms of augmentation type and list. Compared with StandardAug, TrivialAug uses singular augmentation, which improves the performance from 82.52% to 86.33%. Therefore, we verified that a singular augmentation type effectively improves the performance. By comparing StandardAug and our method, we demonstrated that including a context-based image augmentation, Fourier or style, can further enhance the performance to 86.9% and 87.0%, respectively.

Ablation of m in EReplayD: episodically replay sub-datasets can help the generalization. Table 7 shows the results with different sub-sample times in EReplayD. We tried m from 1 to 5 and we found that setting m to 3 can achieve the best performance. In particular, our method can achieve 1.5% improvement over the model without EReplayD ($m = 1$).

Compare EReplayD with traditional ensemble. Table 8 shows the effectiveness of EReplayD. A traditional ensemble refers to train m networks on a whole dataset and ensemble the predictions from m networks as the final result. From Table 8 we can see that our proposed EReplayD, *i.e.*, ensemble by periodically sub-sampling, outperforms the traditional model ensemble method by 1.33%. The result verified the effectiveness of our main assumption, that is, to focus more on learning subsets (sub-datasets).

Table 8: Compare EReplayD with the traditional ensemble on Digits-DG. Note that each experiment ensembles three models.

Ensemble Type	SYN	SVHN	MNIST-M	MNIST	Avg.
Traditional Ensemble	94.93	77.88	71.83	97.95	85.64
EReplayD (ours)	95.33	81.75	72.52	98.28	86.97

4.5 Visualization results

t-SNE visualization. Fig. 4 shows the visualization results of our baseline, FACT [60] and ours. The models are trained on *art_painting*, *photo*, *sketch* and tested on *cartoon*. We can see that our method can better separate the classes on the unseen target domain than the other two methods.

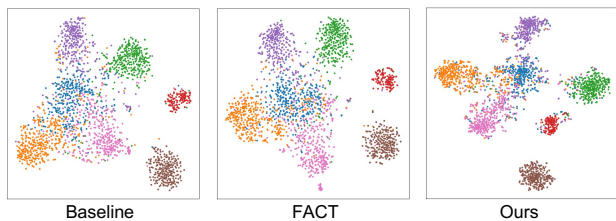


Fig. 4: The t-SNE visualization on *Cartoon* on PACS dataset. Each color represents a class. Bested viewed in color.

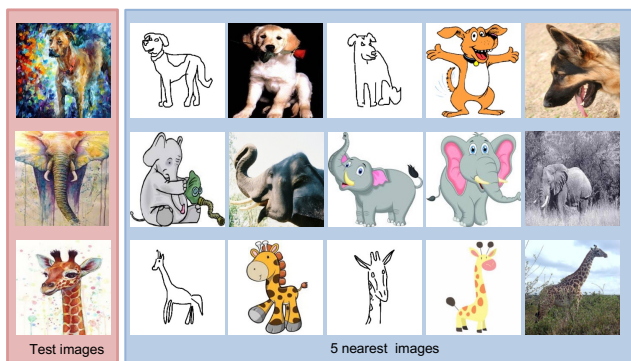


Fig. 5: 5-nearest neighbors for the images from unseen domain (*art_painting*). For each test image, the leftmost image is the closest image from the training dataset (*sketch*, *photo* and *cartoon*).

k -nearest neighbors visualization. Fig. 5 shows the k -nearest neighbors ($k = 5$) for the test image in the unseen domain. We can see that for a test image, the retrieved 5 nearest images from the training dataset

Table 9: Effects of different b and r in EReplayB on Digits-DG.

b and r	SYN	SVHN	MNIST-M	MNIST	Avg.
$b = 4, r = 32$	96.2	79.57	70.12	98.30	86.05
$b = 4, r = 16$	96.45	80.02	70.38	98.42	86.32
$b = 4, r = 8$	95.83	78.60	71.47	98.37	86.07
$b = 4, r = 4$	95.48	81.22	73.15	98.33	87.04
$b = 4, r = 4$	95.48	81.22	73.15	98.33	87.04
$b = 8, r = 4$	96.03	78.45	71.00	98.58	86.02
$b = 16, r = 4$	95.32	79.57	71.02	98.22	86.03
$b = 32, r = 4$	95.52	79.20	69.05	98.30	85.52
$b = 4, r = 4$ (ours)	95.48	81.22	73.15	98.33	87.04

Table 10: Effects of Fourier and Stylization in ESAug on Digits-DG.

	SYN	SVHN	MNIST-M	MNIST	Avg.
Combine Fourier and Stylized	95.45	79.68	73.5	98.43	86.76
TripleE-Fourier	95.33	81.75	72.52	98.28	86.97
TripleE-Stylized	95.48	81.22	73.15	98.33	87.04

have the same semantic information with the test image. The result demonstrates that our method can learn the domain-invariant features and has good model generalization ability.

5 Discussion

5.1 Analysis on different b and r in EReplayB.

Table 9 shows the results with different b and r on Digits-DG. We can see that with a fixed batch size b , the performance improvement is limited when repeat times r increase. The result shows that a high repeat time may not be necessary, and the result reaches the best performance when $r = 4$. On the other hand, when $r = 4$, as b increases, the performance worsens, and the best result is achieved at $b = 4$ and $r = 4$.

5.2 Effects of combining Fourier and stylization in ESAug.

Table 10 shows the results of combining Fourier and stylization in ESAug. We can see that adding both Fourier and Stylized transform achieves 86.76% performance, indicating that these two context-based augmentations have similar effects for model generalization. Therefore, in this paper, we present the results generated by Fourier-based and stylized augmentation individually.

Table 11: Effects of different augmentation probabilities in EAUG on Digits-DG.

	Aug prob.	SYN	SVHN	MNIST-M	MNIST	Avg.
Fourier	1/2	95.47	76.97	69.37	98.03	84.96
stylized	1/2	95.75	75.67	69.53	98.08	84.76
Fourier(ours)	1/15	95.33	81.75	72.52	98.28	86.97
stylized(ours)	1/15	95.48	81.22	73.15	98.33	87.04

5.3 Effects of different augmentation probabilities in ESAUG

We include Fourier-based augmentation/ stylized augmentation into the standard augmentation list, consisting of 14 transformation functions. We studied different probabilities to include these context-exchange augmentations. Table 11 shows that concatenating the context-exchange augmentation (Fourier/Stylized) with the standard augmentation list achieves the best overall performance.

Data availability The six datasets analyzed during the current study are available on the following websites: PACS ², Digits-DG ³, Office-Home ⁴, VLCS ⁵, TerraInc ⁶, DomainNet ⁷.

6 Conclusion

This paper presents a frustratingly easy yet should-know method for domain generalization. Unlike prior work that relies on a particular module, loss function, or structure design, our method is based on simple augmentations and ensembling. We reveal the key secret for model improvement is to encourage the network to train on subsets and enlarge the data space in learning on subsets. Our TripleE achieves this goal through three components: EReplayB, EReplayD, and ESAUG. Experiments demonstrated that TripleE is outperforming or comparable to the state of the art, showing it could serve as a stepping stone for future research in domain generalization.

² <https://drive.google.com/drive/folders/1SKvzI8bCqW9bcoNLNcrTGbg7gBSw97q0>

³ https://drive.google.com/uc?id=15V7EsHfCcfbKgsDmzQKj_DfXt_XYp_P7

⁴ <https://drive.google.com/file/d/0B81rNlvomiwed0V1YUxQdC1u0Tg/view?resourcekey=0-2SNWqQCDauWOBRRBL7ZZsw>

⁵ https://drive.google.com/uc?id=1skwblH1_0kBwxWxmRsp9_qi15hyPpxg8

⁶ https://lilablobssc.blob.core.windows.net/caltechcameratraps/eccv_18_all_images_sm.tar.gz

⁷ <http://ai.bu.edu/M3SDA/>

References

1. Yogesh Balaji, Swami Sankaranarayanan, Rama Chellappa, et al. Metareg: Towards domain generalization using meta-regularization. In *NeurIPS*, pages 998–1008, 2018.
2. Sara Beery, Grant Van Horn, and Pietro Perona. Recognition in terra incognita. In *ECCV*, pages 456–473, 2018.
3. Fabio M. Carlucci, Antonio D’Innocente, Silvia Bucci, Barbara Caputo, and Tatiana Tommasi. Domain generalization by solving jigsaw puzzles. In *CVPR*, June 2019.
4. Junbum Cha, Sanghyuk Chun, Kyungjae Lee, Han-Cheol Cho, Seunghyun Park, Yunsung Lee, and Sungrae Park. Swad: Domain generalization by seeking flat minima. In *NeurIPS*, volume 34, pages 22405–22418, 2021.
5. Junbum Cha, Kyungjae Lee, Sungrae Park, and Sanghyuk Chun. Domain generalization by mutual-information regularization with pre-trained models. *arXiv preprint arXiv:2203.10789*, 2022.
6. Prithvijit Chattopadhyay, Yogesh Balaji, and Judy Hoffman. Learning to balance specificity and invariance for in and out of domain generalization. *ECCV*, 2020.
7. Yang Chen, Yu Wang, Yingwei Pan, Ting Yao, Xinmei Tian, and Tao Mei. A style and semantic memory mechanism for domain generalization. In *ICCV*, pages 9164–9173, 2021.
8. Ekin D Cubuk, Barret Zoph, Dandelion Mane, Vijay Vasudevan, and Quoc V Le. Autoaugment: Learning augmentation strategies from data. In *CVPR*, pages 113–123, 2019.
9. Ekin D Cubuk, Barret Zoph, Jonathon Shlens, and Quoc V Le. Randaugment: Practical automated data augmentation with a reduced search space. In *Proceedings of the IEEE/CVF Conference on Computer Vision and Pattern Recognition Workshops*, pages 702–703, 2020.
10. Qi Dou, Daniel Coelho de Castro, Konstantinos Kamnitsas, and Ben Glocker. Domain generalization via model-agnostic learning of semantic features. In *NeurIPS*, pages 6450–6461, 2019.
11. Antonio D’Innocente and Barbara Caputo. Domain generalization with domain-specific aggregation modules. In *German Conference on Pattern Recognition*, pages 187–198. Springer, 2018.
12. Chen Fang, Ye Xu, and Daniel N Rockmore. Unbiased metric learning: On the utilization of multiple datasets and web images for softening bias. In *ICCV*, pages 1657–1664, 2013.
13. Yaroslav Ganin and Victor Lempitsky. Unsupervised domain adaptation by backpropagation. In *ICML*, pages 1180–1189. PMLR, 2015.
14. Yaroslav Ganin, Evgeniya Ustinova, Hana Ajakan, Pascal Germain, Hugo Larochelle, François Laviolette, Mario Marchand, and Victor Lempitsky. Domain-adversarial training of neural networks. *The Journal of Machine Learning Research*, 17(1):2096–2030, 2016.
15. Alberto Garcia-Garcia, Sergio Orts-Escolano, Sergiu Oprea, Victor Villena-Martinez, and Jose Garcia-Rodriguez. A review on deep learning techniques applied to semantic segmentation. *arXiv preprint arXiv:1704.06857*, 2017.
16. Muhammad Ghifary, W Bastiaan Kleijn, Mengjie Zhang, and David Balduzzi. Domain generalization for object recognition with multi-task autoencoders. In *CVPR*, pages 2551–2559, 2015.
17. Ian Goodfellow, Jean Pouget-Abadie, Mehdi Mirza, Bing Xu, David Warde-Farley, Sherjil Ozair, Aaron Courville,

- and Yoshua Bengio. Generative adversarial nets. In *NeurIPS*, pages 2672–2680, 2014.
18. Ishaan Gulrajani and David Lopez-Paz. In search of lost domain generalization. *arXiv preprint arXiv:2007.01434*, 2020.
 19. Kaiming He, Xiangyu Zhang, Shaoqing Ren, and Jian Sun. Deep residual learning for image recognition [c]. In *CVPR*, volume 2016, pages 770–778, 2016.
 20. Dan Hendrycks, Norman Mu, Ekin D Cubuk, Barret Zoph, Justin Gilmer, and Balaji Lakshminarayanan. Augmix: A simple data processing method to improve robustness and uncertainty. *arXiv preprint arXiv:1912.02781*, 2019.
 21. Elad Hoffer, Tal Ben-Nun, Itay Hubara, Niv Giladi, Torsten Hoefer, and Daniel Soudry. Augment your batch: Improving generalization through instance repetition. In *CVPR*, pages 8129–8138, 2020.
 22. Gao Huang, Zhuang Liu, Laurens Van Der Maaten, and Kilian Q Weinberger. Densely connected convolutional networks. In *CVPR*, pages 4700–4708, 2017.
 23. Xun Huang and Serge Belongie. Arbitrary style transfer in real-time with adaptive instance normalization. In *ICCV*, pages 1501–1510, 2017.
 24. Zeyi Huang, Haohan Wang, Eric P Xing, and Dong Huang. Self-challenging improves cross-domain generalization. *ECCV*, 2020.
 25. Nitish Shirish Keskar, Dheevatsa Mudigere, Jorge Nocedal, Mikhail Smelyanskiy, and Ping Tak Peter Tang. On large-batch training for deep learning: Generalization gap and sharp minima. In *ICLR*, 2017.
 26. Prannay Khosla, Piotr Teterwak, Chen Wang, Aaron Sarna, Yonglong Tian, Phillip Isola, Aaron Maschinot, Ce Liu, and Dilip Krishnan. Supervised contrastive learning. *NeurIPS*, 33:18661–18673, 2020.
 27. Daehee Kim, Youngjun Yoo, Seunghyun Park, Jinkyu Kim, and Jaekoo Lee. Selfreg: Self-supervised contrastive regularization for domain generalization. In *ICCV*, pages 9619–9628, 2021.
 28. Yann LeCun, Léon Bottou, Yoshua Bengio, and Patrick Haffner. Gradient-based learning applied to document recognition. *Proceedings of the IEEE*, 86(11):2278–2324, 1998.
 29. Da Li, Yongxin Yang, Yi-Zhe Song, and Timothy M Hospedales. Deeper, broader and artier domain generalization. In *ICCV*, pages 5542–5550, 2017.
 30. Da Li, Yongxin Yang, Yi-Zhe Song, and Timothy M Hospedales. Learning to generalize: Meta-learning for domain generalization. *AAAI*, 2018.
 31. Da Li, Jianshu Zhang, Yongxin Yang, Cong Liu, Yi-Zhe Song, and Timothy M. Hospedales. Episodic training for domain generalization. In *ICCV*, October 2019.
 32. Haoliang Li, Sinno Jialin Pan, Shiqi Wang, and Alex C Kot. Domain generalization with adversarial feature learning. In *CVPR*, pages 5400–5409, 2018.
 33. Pan Li, Da Li, Wei Li, Shaogang Gong, Yanwei Fu, and Timothy M Hospedales. A simple feature augmentation for domain generalization. In *ICCV*, pages 8886–8895, 2021.
 34. Xiaomeng Li, Hao Chen, Xiaojuan Qi, Qi Dou, Chi-Wing Fu, and Pheng-Ann Heng. H-denseunet: hybrid densely connected unet for liver and tumor segmentation from ct volumes. *IEEE transactions on medical imaging*, 37(12):2663–2674, 2018.
 35. Ya Li, Xinmei Tian, Mingming Gong, Yajing Liu, Tongliang Liu, Kun Zhang, and Dacheng Tao. Deep domain generalization via conditional invariant adversarial networks. In *ECCV*, pages 624–639, 2018.
 36. Yi Li, Haozhi Qi, Jifeng Dai, Xiangyang Ji, and Yichen Wei. Fully convolutional instance-aware semantic segmentation. In *CVPR*, pages 2359–2367, 2017.
 37. Sungbin Lim, Ildoo Kim, Taesup Kim, Chiheon Kim, and Sungwoong Kim. Fast autoaugment. In *NeurIPS*, page 32, 2019.
 38. Massimiliano Mancini, Zeynep Akata, Elisa Ricci, and Barbara Caputo. Towards recognizing unseen categories in unseen domains. *arXiv preprint arXiv:2007.12256*, 2020.
 39. Dominic Masters and Carlo Luschi. Revisiting small batch training for deep neural networks. *arXiv preprint arXiv:1804.07612*, 2018.
 40. Toshihiko Matsuura and Tatsuya Harada. Domain generalization using a mixture of multiple latent domains. In *AAAI*, pages 11749–11756, 2020.
 41. Saeid Motiian, Marco Piccirilli, Donald A Adjeroh, and Gianfranco Doretto. Unified deep supervised domain adaptation and generalization. In *ICCV*, pages 5715–5725, 2017.
 42. Samuel G Müller and Frank Hutter. Trivialaugment: Tuning-free yet state-of-the-art data augmentation. In *ICCV*, pages 774–782, 2021.
 43. Yuval Netzer, Tao Wang, Adam Coates, Alessandro Bisacco, Bo Wu, and Andrew Y Ng. Reading digits in natural images with unsupervised feature learning. 2011.
 44. Oren Nuriel, Sagie Benaim, and Lior Wolf. Permuted adain: reducing the bias towards global statistics in image classification. In *CVPR*, pages 9482–9491, 2021.
 45. Henri J Nussbaumer. The fast fourier transform. In *Fast Fourier Transform and Convolution Algorithms*, pages 80–111. Springer, 1981.
 46. Adam Paszke, Sam Gross, Francisco Massa, Adam Lerer, James Bradbury, Gregory Chanan, Trevor Killeen, Zeming Lin, Natalia Gimelshein, Luca Antiga, Alban Desmaison, Andreas Kopf, Edward Yang, Zachary DeVito, Martin Raison, Alykhan Tejani, Sasank Chilamkurthy, Benoit Steiner, Lu Fang, Junjie Bai, and Soumith Chintala. Pytorch: An imperative style, high-performance deep learning library. In H. Wallach, H. Larochelle, A. Beygelzimer, F. d'Alché-Buc, E. Fox, and R. Garnett, editors, *NeurIPS*, pages 8024–8035. Curran Associates, Inc., 2019.
 47. Xingchao Peng, Qinxun Bai, Xide Xia, Zijun Huang, Kate Saenko, and Bo Wang. Moment matching for multi-source domain adaptation. In *ICCV*, pages 1406–1415, 2019.
 48. Shiv Shankar, Vihari Piratla, Soumen Chakrabarti, Sidhartha Chaudhuri, Preethi Jyothi, and Sunita Sarawagi. Generalizing across domains via cross-gradient training. *ICLR*, 2018.
 49. Baifeng Shi, Dinghui Zhang, Qi Dai, Zhanxing Zhu, Yadong Mu, and Jingdong Wang. Informative dropout for robust representation learning: A shape-bias perspective. *ICML*, 2020.
 50. Yuge Shi, Jeffrey Seely, Philip HS Torr, N Siddharth, Awni Hannun, Nicolas Usunier, and Gabriel Synnaeve. Gradient matching for domain generalization. In *ICLR*, 2022.
 51. Nathan Somavarapu, Chih-Yao Ma, and Zsolt Kira. Frustratingly simple domain generalization via image stylization. *arXiv preprint arXiv:2006.11207*, 2020.
 52. Nitish Srivastava, Geoffrey Hinton, Alex Krizhevsky, Ilya Sutskever, and Ruslan Salakhutdinov. Dropout: a simple way to prevent neural networks from overfitting. *The journal of machine learning research*, 15(1):1929–1958, 2014.

53. Baochen Sun and Kate Saenko. Deep coral: Correlation alignment for deep domain adaptation. In *ECCV*, pages 443–450. Springer, 2016.
54. Hemanth Venkateswara, Jose Eusebio, Shayok Chakraborty, and Sethuraman Panchanathan. Deep hashing network for unsupervised domain adaptation. In *CVPR*, pages 5018–5027, 2017.
55. Riccardo Volpi, Hongseok Namkoong, Ozan Sener, John C Duchi, Vittorio Murino, and Silvio Savarese. Generalizing to unseen domains via adversarial data augmentation. In *NeurIPS*, pages 5334–5344, 2018.
56. Haohan Wang, Songwei Ge, Zachary Lipton, and Eric P Xing. Learning robust global representations by penalizing local predictive power. In *NeurIPS*, pages 10506–10518, 2019.
57. Haohan Wang, Zexue He, Zachary C Lipton, and Eric P Xing. Learning robust representations by projecting superficial statistics out. In *ICLR*, 2019.
58. Shujun Wang, Lequan Yu, Caizi Li, Chi-Wing Fu, and Pheng-Ann Heng. Learning from extrinsic and intrinsic supervisions for domain generalization. *ECCV*, 2020.
59. Yunqi Wang, Furui Liu, Zhitang Chen, Qing Lian, Shoubo Hu, Jianye Hao, and Yik-Chung Wu. Contrastive ace: Domain generalization through alignment of causal mechanisms. *arXiv preprint arXiv:2106.00925*, 2021.
60. Qinwei Xu, Ruipeng Zhang, Ya Zhang, Yanfeng Wang, and Qi Tian. A fourier-based framework for domain generalization. In *CVPR*, pages 14383–14392, 2021.
61. Xiangyu Yue, Yang Zhang, Sicheng Zhao, Alberto Sangiovanni-Vincentelli, Kurt Keutzer, and Boqing Gong. Domain randomization and pyramid consistency: Simulation-to-real generalization without accessing target domain data. In *ICCV*, pages 2100–2110, 2019.
62. Sergey Zakharov, Wadim Kehl, and Slobodan Ilic. Deceptionnet: Network-driven domain randomization. In *ICCV*, pages 532–541, 2019.
63. Kaiyang Zhou, Yongxin Yang, Timothy Hospedales, and Tao Xiang. Deep domain-adversarial image generation for domain generalisation. In *AAAI*, volume 34, pages 13025–13032, 2020.
64. Kaiyang Zhou, Yongxin Yang, Timothy Hospedales, and Tao Xiang. Learning to generate novel domains for domain generalization. In *ECCV*, pages 561–578. Springer, 2020.
65. Kaiyang Zhou, Yongxin Yang, Yu Qiao, and Tao Xiang. Domain generalization with mixstyle. *arXiv preprint arXiv:2104.02008*, 2021.
66. Zongwei Zhou, Md Mahfuzur Rahman Siddiquee, Nima Tajbakhsh, and Jianming Liang. Unet++: A nested u-net architecture for medical image segmentation. In *Deep Learning in Medical Image Analysis and Multimodal Learning for Clinical Decision Support*, pages 3–11. Springer, 2018.